FEBS Letters 580 (2006) 2087–2091

Recapture of [S]-allantoin, the product of the two-step degradation of uric acid, by urate oxidase

Laure Gabison[a], Mohamed Chiadmi[a], Nathalie Colloc'h[b], Bertrand Castro[c], Mohamed El Hajji[c], Thierry Prangé[a,*]

[a] *Laboratoire de cristallographie et RMN biologiques (UMR 8015 CNRS), Faculté de Pharmacie, Université Paris V, 4 avenue de l'Observatoire, 75270 Paris Cedex 06, France*
[b] *UMR 6185 CNRS, Université de Caen, Centre Cyceron, Bd Becquerel, BP 5229, 14074 Caen Cedex, France*
[c] *SANOFI-AVENTIS Recherche & Développement, Rue du Pr Blayac, 34184 Montpellier, France*

Received 19 December 2005; revised 7 February 2006; accepted 1 March 2006

Available online 10 March 2006

Edited by Hans Eklund

Abstract **Urate oxidase from *Aspergillus flavus* catalyzes the degradation of uric acid to [S]-allantoin through 5-hydroxyisourate as a metastable intermediate. The second degradation step is thought either catalyzed by another specific enzyme, or spontaneous. The structure of the enzyme was known at high resolution by X-ray diffraction of *I*222 crystals complexed with a purine-type inhibitor (8-azaxanthin). Analyzing the X-ray structure of urate oxidase treated with an excess of urate, the natural substrate, shows unexpectedly that the active site recaptures [S]-allantoin from the racemic end product of a second degradation step.**

Keywords: Urate oxidase; Uricase; Allantoin; 8-Azaxanthin; 5-Hydroxyisourate; *Aspergillus flavus*

1. Introduction

Urate oxidase (uricase; EC 1.7.3.3; or UOX) is a 135 kDa tetrameric enzyme of therapeutic interest implicated in the catalysed degradation of uric acid (Scheme 1). It catalyzes the first step of the degradation of uric acid **1** to 5-hydroxyisourate (5-HIU) **2**. The second degradation step leads to [S]-allantoin **3** (or [S]-ALN). UOX from *Aspergillus flavus* gene, cloned in a *Saccharomyces cerevisiae* strain, is produced by Sanofi-Aventis according to a patented process.

The first three-dimensional structure of extracted UOX was solved at a resolution of 2.05 Å in complex with 8-azaxanthin (8-AZA), a stabilizing inhibitor [1] in the *I*222 orthorhombic form. Following this first report and the preparation of recombinant UOX, several more accurate structures, in complex with 9-methyl urate or oxonate became available [2]. High-diffraction properties of the resulting diamond-shaped *I*222 crystals confirmed that these molecules were good analogues. Moreover, the structure of the ligand-free enzyme solved from a monoclinic form ($P2_1$) was also described as well as other polymorphs using the less analogous uracil or guanine as ligands [3] but diffracting at lower resolution. All these purine-type inhibitors share the same –NH(3)–CO(2)–NH(1)–CO(6)– motif in their six-membered ring. Other close compounds like cafein, theobromin or theophyllin whose NH are methylated, do not interact with UOX [4]. When ligand-free UOX crystals are soaked in a urate-containing solution, they immediately crack and dissolve, as a result of conformational changes during the in situ catalytic reaction. To get more information about the catalytic pathway and about the end of the reaction, the enzyme was first set to react in solution with urate, then set to crystallize afterwards. In all cases, the complex leads to the formation of the high resolution *I*222 orthorhombic crystals, an indication that stabilization occurs within the active site at the end of the reaction prior to crystallization. The present study aims at characterizing the content of the protein at that time.

2. Materials and methods

2.1. Crystallizations

Purified recombinant UOX from *A. flavus*, expressed in *S. cerevisiae*, was supplied by Sanofi-Aventis. All additives and chemicals used in this study (uric acid, polyethyleneglycol, etc.) were purchased from Sigma–Aldrich. The enzyme was incubated at a concentration of 15 mg/mL at pH 8.5 with an excess of uric acid (0.5–2 mg/mL). The solution was immediately set to crystallize following identical crystal growth conditions as previously described using the sitting-drop vapor diffusion method at room temperature [5]. 5–10 mg/mL protein in 50 mM Tris/HCl pH 8.5 in the presence of 5–8% w/v PEG 8000 and NaCl 0.05 M, led to orthorhombic crystals within 24–48 h. They grow to their full extension (~0.6 mm) within a week.

2.2. X-ray data collection and data processing

X-ray data collections were carried out at the ESRF BM14 beamline, at a wavelength of 0.972 Å and operating in a 16 bunch mode, using a MAR CCD detector; temperature was set to 277 K. Data were integrated by DENZO and scaled independently using SCALEPACK, both software are parts of the HKL package [6]. Cell parameters were refined by the post-refinement technique implemented in SCALEPACK. The merged intensity data were converted to structure-factor amplitudes by TRUNCATE [7] and put on an approximate absolute scale using the scale factor taken from a Wilson plot computed with data in the resolution range of 5 Å – d_{min} (see statistics in Table 1).

*Corresponding author. Address: Laboratoire de cristallographie et RMN biologiques, Faculté de pharmacie, 4 Ave de l'Observatoire, 75006 Paris, France. Fax: +33 1 53 73 99 25.
E-mail address: thierry.prange@univ-paris5.fr (T. Prangé).

Abbreviations: UOX, urate oxidase; 8-AZA, 8-azaxanthin; [S]-ALN, [S]-allantoin; 5-HIU, 5-hydroxyisourate; RMSD, root mean squares deviation

0014-5793/$32.00
doi:10.1016/j.febslet.2006.03.007

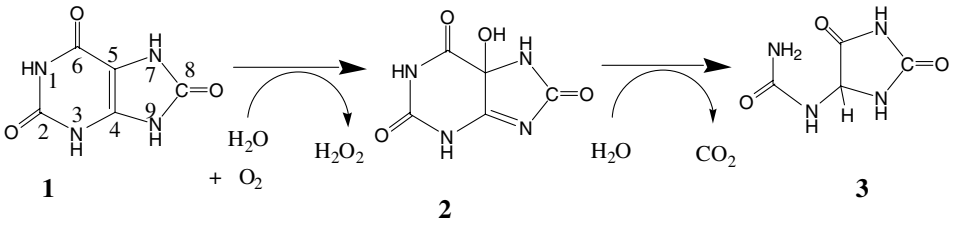

Scheme 1.

2.3. Protein structure solution

The structure was solved by Fourier synthesis using the calculated phases derived from the isomorphous structure taken from the Protein Data Bank (code 1R51 or 1R4S) after removing all the water molecules and the ligand.

Table 1
Data collection and refinements statistics

Data collection	
Space group	*I*222
Parameters (Å)	
a	80.36
b	96.09
c	105.37
Number of unique reflections	39454
Data redundancy	4.8
All data (10.9–1.75 Å)	
R_{sym} (%)	6.4
Mean $I/\sigma(I)$	18.7
Overall completeness (%)	98.1
Highest resolution shell (2.1–2.0 Å)	
R_{sym} (%)	28.7
Mean $I/\sigma(I)$	5.1
Completeness (%)	97.6
Refinements (SHELXL)	
Number of atoms	
UOX	2384
[S]-ALN	11
Solvent (H_2O)	168
Resolution range (Å)	10–1.76
Number of parameters/restraints	10259/9887
R factor (%), for 4σ observed data (number)	19.1 (33270)
R factor (%), for all data (number)	20.8 (39227)
Free *R* factor (%) for 7% of obs. data (number)	23.0 (2758)

	Value
Mean isotropic $\langle B \rangle$ values (Å^2)	
Main chain	18.7
Side chain	25.6
Water molecules	35.9
[S]-allantoin	28.0
Residuals in final Fourier map (min/max) (e$^-$)	−0.25/+0.40

RMS deviations	Number	Target/value
1–2 Bond length (Å)	2451	0.03/0.034
1–3 Bond-distance angles (Å)	3321	0.08/0.077
Planes (Å)	790	0.4/0.35
Non-zero chiral volumes (Å^3)	369	0.1/0.045

The structure refinements were carried out with the program SHELXL [8]. Throughout the course of refinements, 7% of the data was left out for cross validation (*R*-free).

The first SIGMAA 2$|F_o-F_c|$ map revealed the presence of an elongated density in the active site accurate enough to be readily shaped as [S]-allantoin. Subsequent maps were checked to remove significant errors in the model, and manual rebuildings were performed using the program O [9]. Alternations of rounds of positional plus restrained *B*-factor refinements followed by manual rebuilding using O were performed until model completion, including successive locations and refinements of water molecules. Final statistics on the model parameter refinements are given in Table 1. Coordinates are deposited with the Protein Data Bank (PDB code: 2FXL). Fig. 1 typically represents a $2F_o-F_c$ map around the ligand, located in the active site.

3. Results and discussion

Strategy for structural studies of an enzymatic mechanism usually aims at trapping the enzyme both in the ground- and transition states, using in the latter case inhibitors that mimic the expected geometry. Co-crystallization with the substrate analogs becomes a mandatory stage to line out the enzyme active site in its stable ground state. For that purpose, analogues that closely resemble uric acid, the natural substrate were pre-

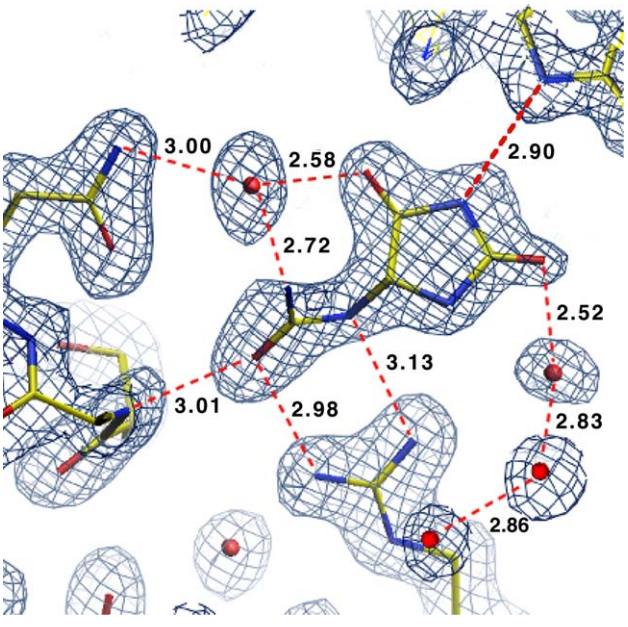

Fig. 1. Weighted electron density map of the active site cavity, calculated with theoretical phases, contouring is at 1.8 sigma above the background level. The [S]-ALN molecule is strongly H-bonded to both the side chains lining the active site and the water molecules that build a long spine in the access channel. Almost all the polar atoms of allantoin are involved in its binding scheme.

viously investigated [2,3]. In presence of uric acid, the same high diffracting orthorhombic form was obtained. In this *I*222 crystal form, the whole functional tetrameric enzyme is built from the repetition of one monomer (the fourth of the enzyme) following the crystallographic 222 symmetry with two different interfaces [3]. The functional tetramer forms a large 16 β-stranded barrel termed *Tunneling-fold* [1], a new motif now shared by several other classes of enzymes [10]. The active site is located at the interface of two subunits. The components of the reaction center are a molecular tweezers (Arg176, Gln 228), a "platform" (Phe 159) and a "water holder" triad (Asn 254, Thr 57*, and Lys 10*, from a second subunit). Numerous water molecules are associated with these residues, and especially what is expected to be the catalytic water (W1) maintained in place 3 Å above the C4–C5 double bond of the substrate by the "water holder". Mutations of these residues invariably result in a drastic loss in the catalytic reaction rate [11,12].

The catalytic mechanism of uric acid oxidation by UOX is complex. Many studies have been done and are still on going to understand how this oxidase works without any cofactor or metal ion. Isotopic experiments have shown that oxygen atom from hydrogen peroxide derived from molecular oxygen and that carbon dioxide derived from the C6 of uric acid [13]. Given the p*K* value of the four acid groups of uric acid, it is likely that a dianion, as initially proposed by Bentley and Neuberger [13], would be the actual substrate. Which dianion is effective is presently unclear, the N3,N9 dianion has been first proposed [14,15] but a N3,N7 dianion may be equally advocated [16]. Allantoin is the ultimate product of the reaction. However, NMR [17] and spectroscopy [18,19] studies suggested that a metastable intermediate, identified as 5-HIU, was the real product of the reaction. Other short-life intermediates, amongst them a hydroperoxide, between urate dianion and 5-HIU have been proposed through stopped-flow absorbance and fluorescence spectroscopy experiments [19,20]. However, according to another mechanism from quantum mechanistic calculations, no hydroperoxide intermediate needs to be postulated [16]. Mutagenesis studies in *B. subtilis* have shown that a threonine and a lysine (T57 and K10 in *A. flavus* UOX numbering, both implicated in the "water holder") play a role in the catalytic reaction, while the neighbor aspartic acid D58 does not [11]. The Phe 159, 3.5 Å below the planar ligand, is also of great importance by stacking (and hence stabilizing) the dianion [12]. Still under investigation is the end of the reaction (step **2** to **3** in Scheme 1). Initially stated as a non-enzymatic and spontaneous hydrolysis without implication of UOX, this last step is now thought accelerated by another enzyme not fully characterized [21–23].

3.1. Allantoin in the active site

The Fig. 2 represents the superimposition of the active site environment in two different structures: 8-AZA/UOX vs [S]-ALN/UOX. All the mandatory partners are represented: the molecular tweezers (Arg 176 and Gln 228), the triad Asn 254, Thr 57* and Lys 10*, and the platform Phe 159. The W1 water molecule held by the triad is observed in all the structures of UOX so far determined [1–3] in a location that invoke the premises of the hydroxylation step of the reaction. In all the UOX/inhibitor complexes, the ligand adopt the same orientation at the same place, a strong indication that urate would certainly benefit of the same location at the beginning of the catalysis. Surprisingly, UOX accommodates also [S]-ALN at the exact location of 8-AZA showing only a slight rotation (Fig. 2B) about the five-membered ring. This illustrates an unexpected plasticity of the UOX active site as it can accommodate not only the well known cyclic purine NH–CO–NH–CO– motif but also open ring compounds like allantoin. In this complex, all the N and O atoms are involved in strong polar interactions toward either the protein and/or

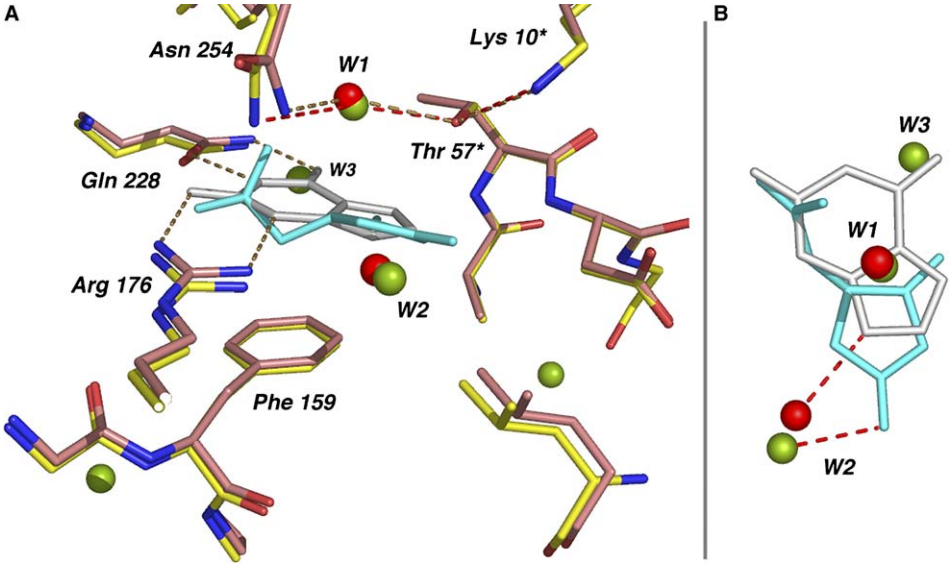

Fig. 2. (A) Superimposition of the active sites of [S]-ALN/UOX and 8-AZA/UOX. The [S]-ALN ligand is shown in cyan and 8-AZA in grey. Only water molecules of interest are represented: W1, held by Asn 254 and Thr 57* (* stands for a symmetry-related subunit) with Lys 10* as a relay, and W2 in the mean plane of the ligand. In [S]-ALN/UOX, W3 fills the location of the O(2) atom from 8-AZA and relays the molecular tweezers Arg176/Gln 228 (also visible in Fig. 1). Water molecules are color coded in red for 8-AZA/UOX and in green for [S]-ALN/UOX. (B). Top view of the active site ligands. [S]-ALN and 8-AZA (equivalent to the initial product) display a small restricted rotation in the plane imposed by Phe-159 stacking and a different hydrogen bonding scheme. Cartoons are drawn using PyMol [26], water molecules are color coded like in A.

water relays. The molecular tweezers still hold the ligand but in a non-symmetric manner, due to the cavity now opened by the missing six-membered ring in [S]-ALN. To allow correct hydrogen bonding, Gln 228 now recruits a new water molecule (W3). This W3 molecule is also observed in the ligand-free structure [2]. Important to note is the polar interaction between [S]-ALN and the Thr 57* main chain nitrogen, already observed in all the high resolution *I*222 structures with purine-type inhibitors, and thought to be at the origin of the perfect two-fold symmetry of the orthorhombic form. Above the mean plane of [S]-ALN, the "water holder" triad adopts a looser configuration compared to the 8-AZA/UOX structure. The first interaction in the triad Asn254–W1–Thr57*–Lys10* is nearly abolished as distance increases from 2.78 Å in 8-AZA/UOX up to 3.47 Å in [S]-ALN/UOX complex, due to a clear displacement of Asn 254 side chain of about one angström. However, the W1 molecule, still hydrogen-bonded to the Thr57*, remains in place for a new reaction. The distance between Thr57* and Lys10* side chains is also lengthened of 0.35 Å. Thus only W1 and Thr57* are not spatially affected. In the structure of UOX without inhibitor [2] and, in a lesser extend, in UOX from other sources (*Bacillus* sp. and *Arthrobacter globiformis*, PDB codes: 1J2G, 1VAX, [24,25]), it is always the Asn 254 side chain the most affected in the different active sites. A superimposition of the residue side chains that build the active site in the 8-azaxanthin and the allantoin complexes, shows a RMSD of 0.2 Å with a maximum of 0.6 Å for Asn 254. The W2 molecule, located in the plane near the N(9) of 8-azaxanthin, and probably at close distance of the protonated urate N(9), occupies the same position with respect to allantoin. W2 like W1 is also ready in good place to interact with the substrate.

3.2. Stereochemical implications

According to the overall geometry of the partners, and especially W1 above the urate plane, it is plausible that the absolute configuration of 5-HIU is [S] with the hydroxyl function in axial position. Up to now, the chirality of 5-HIU has not yet been determined. Further degradation of [S]5-HIU would logically drive to [S]-ALN if the molecule stays in a chiral environment. Hence, to explain the formation of the [S]-ALN/UOX complex, two hypotheses may be formulated at the end of the first step of the reaction: either (i) the 5-HIU is expelled, its hydrolysis occurs in solution and the enzyme catch back selectively the [S] isomer from the racemic [±]-ALN in solution, or (ii) the two steps ending to [S]-ALN proceed in the active site of UOX, leading to an optically active [S]-ALN. It is very unlikely that the mechanism follows the second hypothesis according to the numerous experimental and theoretical evidences [16–23]. In that context, the recapture of [S]-ALN is the most probable pathway.

4. Conclusion

In the present study, we report an insight of one end state of urate degradation by UOX. Assuming that 8-AZA position mimics the location of urate, we have in hands two ground states of the enzyme. Indeed, nothing can be determined about the different intermediates that several authors have proposed [15–17,19,20,23]. Because X-ray diffraction offers only a static view of stable configurations, it is difficulty to catch a metastable intermediate with a short lifetime like 5-HIU. However, comparisons between these two states show that the recaptured ligand in the active site keeps the same orientation with a rearrangement of the hydrogen bonding around it. This is also true for the side chains lining the active site. Questions still remain about the end of the degradation and the role and origin of the 5-HIU hydrolase [22,23]. Allantoin itself is further degraded by a specific enzyme to allantoate, a process that requires [S]-ALN as substrate, not the racemic mixture that would result from a non-enzymatic hydrolysis of 5-HIU. With these considerations, 5-HIU hydrolase, although not necessary, becomes an important link to speed up the degradation chain of urate by selecting the good enantiomer. The present observation that UOX is able to catch back the end product with a high affinity reveals unexpected plasticity and conformational adaptation of UOX active site that was not observed before.

Acknowledgments: We thank Sanofi-Aventis for supplying us with pure enzyme, and Martin Walsh, (ESRF, Grenoble, France), for access and advises on the BM14 beam line.

References

[1] Colloc'h, N., El Hajji, M., Bachet, B., L'Hermite, G., Schiltz, M., Prangé, T., Castro, B. and Mornon, J.P. (1997) Crystal structure of the protein drug urate oxidase-inhibitor complex at 2.05 Å resolution. Nat. Struct. Biol. 4, 947–952.
[2] Retailleau, P., Colloc'h, N., Vivarès, D., Bonneté, F., Castro, B., El Hajji, M., Mornon, J.P, Monard, G. and Prangé, T. (2004) Complexed and ligand-free high resolution structures of urate oxidase (Uox) from *Aspergillus flavus*: a reassignment of the active site binding mode. Acta Crystallogr. D 60, 453–462.
[3] Retailleau, P., Colloc'h, N., Vivarès, D., Bonneté, F., Castro, B., El Hajji, M. and Prangé, T. (2005) Urate oxidase from *Aspergillus flavus*: new crystal packing contacts in relation to the content of the active site. Acta Crystallogr. D 61, 218–229.
[4] Laboureur, P. and Langlois, C. (1968) Urate oxydase d'*Aspergillus flavus* II. Métabolisme, inhibitions, spécificité. Bull. Soc. Chim. Biol. 50 (4), 827–837.
[5] Vivarès, D. and Bonneté, F. (2002) X-ray scattering studies of *Aspergillus flavus* urate oxidase: towards a better understanding of PEG effects on the crystallization of large proteins. Acta Crystallogr. D 58, 472–479.
[6] Otwinowski, Z. and Minor, W. (1997) Processing of X-ray diffraction data collected in oscillation mode. Methods Enzymol. 276, 306–326.
[7] Collaborative Computational Project, Number 4 (1994) The CCP4 suite: programs for protein crystallography. Acta Crystallogr. D 50, 760–763.
[8] Sheldrick, G.M. and Schneider, T.R. (1997) SHELXL: High resolution refinement. Methods Enzymol. 277, 319–341.
[9] Jones, T.A., Zou, J.Y., Cowan, S.W. and Kjeldgaard, M. (1991) Improved methods for building protein models in electron density maps and the location of errors in these models. Acta Crystallogr. A 47, 110–119.
[10] Colloc'h, N., Poupon, M. and Mornon, J.P. (2000) Sequence and structural features of the T-fold, an original tunnelling building unit. Proteins 39, 142–154.
[11] Imhoff, R.D., Power, N.P., Borrok, M.J. and Tipton, P.A. (2003) General base catalysis in the urate oxidase reaction: evidence for a novel Thr-Lys catalytic diad. Biochemistry 42, 4094–4100.
[12] Doll, C., Bell, A.F., Power, N., Tonge, P.J. and Tipton, P.A. (2005) Procatalytic ligand strain. Ionization and perturbation of 8-nitroxanthine at the urate oxidase active site. Biochemistry 44, 11440–11446.
[13] Bentley, R. and Neuberger, A. (1952) The mechanism of the action of uricase. Biochem. J. 52, 694–699.

[14] Kahn, K. (1999) Theoretical studies of intermediates in the urate oxidase reaction. Bioorg. Chem. 27, 351–362.
[15] Kahn, K., Serfozo, P. and Tipton, P.A. (1997) Identification of the true product of the urate oxidase reaction. J. Am. Chem. Soc. 119, 5435–5442.
[16] Altarsha, M., Monard, G. and Castro, B. (in press) A comparative semiempirical and ab initio study of the structural and chemical properties of uric acid and its anions. Int. J. Quantum Chem.
[17] Modric, N., Derome, A.E., Ashcroft, S.J.H. and Poje, M. (1992) Tracing and identification of uricase reaction intermediate. Tetrahedron Lett. 33, 6691–6694.
[18] Kahn, K. and Tipton, P.A. (1998) Spectroscopic characterization of intermediates in the urate oxidase reaction. Biochemistry 37, 11651–11659.
[19] Tipton, P.A. (2002) Urate oxidase: single-turnover stopped-flow techniques for detecting two discrete enzyme-bound intermediates. Methods Enzymol. 354, 310–319.
[20] Sarma, A.D. and Tipton, P.A. (2000) Evidence for urate hydroperoxide as an intermediate in the urate oxidase reaction. J. Am. Chem. Soc. 122, 11252–11253.
[21] Raychaudhuri, A. and Tipton, P.A. (2003) A familiar motif in a new context: the catalytic mechanism of hydroxyisourate hydrolase. Biochemistry 42, 6848–6852.
[22] Sarma, A.D., Serfozo, P., Kahn, K. and Tipton, P.A. (1999) Identification and purification of hydroxyisourate hydrolase, a novel ureide-metabolizing enzyme. J. Biol. Chem. 274, 33863–33865.
[23] Lee, Y., Lee, D.H., Kho, C.W., Lee, A.Y., Jang, M., Cho, S., Lee, C.H., Lee, J.S., Myung, P.K., Park, B.C. and Park, S.G. (2005) Transthyretin-related proteins function to facilitate the hydrolysis of 5-hydroxyisourate, the end product of the uricase reaction. FEBS Lett. 579, 4769–4774.
[24] Hibi, T., Nago, T., Nishiya, Y. and Oda, J. (2004) Protein Data Bank, Code: 1J2G.
[25] Hossain, M.T., Juan, E.C.M., Suzuki, K., Yamanoto, T., Imamura, S., Sekiguchi, T. and Takenaka, A. (2005) Protein Data Bank, Codes: 1VAX, 1VAY.
[26] DeLano, W.L. (2002) The PyMOL Molecular Graphics System. DeLano Scientific, San Carlos, CA, USA. Available from: http://www.pymol.org.